

TRACKING A MOBILE NODE BY ASYNCHRONOUS NETWORKS

Yiyin Wang*, Geert Leus*, and Xiaoli Ma†

* Delft University of Technology, Fac. EEMCS, Mekelweg 4, 2628CD Delft, The Netherlands

† School of ECE, Georgia Institute of Technology, Atlanta, GA 30332-0250, USA

ABSTRACT

In this paper, we propose a Kalman filter (KF) based tracking approach to track a target node with the assistance of anchors in an asynchronous network with clock offsets. We employ the asymmetric trip ranging (ATR) protocol to obtain TOA measurements and facilitate clock offset cancellation, and further derive a linear measurement model from the TOA measurements. Thus, the KF based on this linear measurement model does not have the modeling errors inherently contained in the Extended Kalman filter (EKF). Furthermore, low computational complexity makes the proposed KF a promising solution for practical use. We compare the proposed KF with the EKF. The simulation results corroborate its efficiency.

Index Terms— Tracking, synchronization, sensor network, time-of-arrival(TOA), clock offset, Kalman filter

1. INTRODUCTION

Tracking a mobile target node is an important issue in many wireless sensor network (WSN) applications [1, 2, 3]. In general, tracking systems follow two steps. In the first step, metrics bearing location information are measured, such as time-of-arrival (TOA) or time-difference-of-arrival (TDOA), angle-of-arrival (AOA), and received signal strength (RSS) [4]. High accuracy and potentially low cost implementation make TOA or TDOA based on ultra-wideband impulse radios (UWB-IRs) a promising ranging method [4]. Consequently, clock synchronization has to be taken into account for a localization or a tracking system using TOA or TDOA measurements [2, 3, 5]. In the second step, the ranging measurements are used to track the target position. Due to the nonlinear relations between these ranging measurements and the coordinates of the mobile target node, the conventional Kalman filter (KF) can not be used. The extended Kalman filter (EKF) [6] is most widely used to linearize the non-linear model. However, the performance of the EKF is decided by how well the linear approximation is. Furthermore, the unscented Kalman filter (UKF) [7] is proposed to overcome the drawbacks of

the EKF. The UKF follows the principle that it is easier to approximate a probability distribution than a random nonlinear model, and it calculates the stochastic properties of a random variable undergoing a nonlinear transformation. Moreover, the particle filter [8] is also a powerful tool to deal with nonlinear models and non-Gaussian noise for tracking. However, both the UKF and the particle filter are computationally intensive. An EKF and a UKF are proposed in [2] to track a target node with fixed anchors (nodes with known positions) in asynchronous networks with clock skews and clock offsets. The target node periodically transmits a pulse. The TDOAs of these pulses received by the same anchor are calculated in order to cancel the anchor clock offset. Then the impact of the clock skews on the TDOAs is approximated as a zero mean Gaussian noise term. However, in practice the variation of the clock skew is observed by hours [9], and should thus be viewed as a random variable with an unknown mean rather than a zero mean random variable. A sequential Monte Carlo (SMC) method is proposed in [3] to jointly estimate the clock offsets and the target trajectory for asynchronous WSNs, which is also computationally intensive.

In this paper, a KF based tracking method is developed to track the target node position with the help of anchors in asynchronous networks with clock offsets. Our work is inspired by [10], where pseudomeasurements linear to the state are constructed based on conventional ranging measurements, and a KF is proposed based on the linear model. But [10] only discusses a scenario, which is composed of three anchor nodes and one target. We consider asynchronous networks with clock offsets among the anchors, and no synchronization requirement for the target node. The asymmetric trip ranging (ATR) protocol proposed in [5] is employed here to obtain TOA measurements and facilitate clock offset cancellation. Since all the TOA measurements are obtained at the anchors, our KF tracker can avoid any influence of the asynchronous target clock. Consequently, a linear measurement model is derived from the TOA measurements via projection and element-wise multiplication. This exact linearization is different from the first order approximation of the EKF. Thus, the KF based on this linear measurement model does not have the modeling errors inherently contained in the EKF. Furthermore, low computational complexity makes the proposed KF a promising solution for practical use. We com-

This research was supported in part by STW under the Green and Smart Process Technologies Program (Project 7976); X. Ma was supported in part by the Georgia Tech Ultra-wideband Center of Excellence (<http://www.uwbtech.gatech.edu/>).

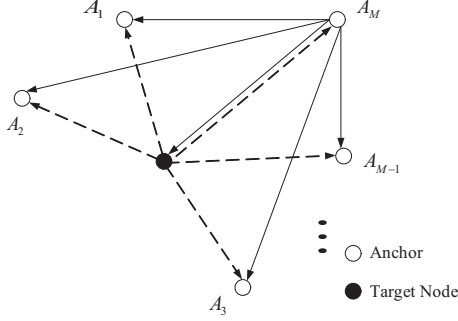


Fig. 1. An example of the ATR protocol for static asynchronous networks

pare the proposed KF with the EKF by simulations. In future work, we would like to propose low complexity trackers for asynchronous WSNs not only with clock offsets but also with clock skews.

2. LINEARIZATION OF THE MEASUREMENT MODEL

For simplicity, we consider M anchors and one target node. We assume that all nodes are distributed in an l -dimensional space, e.g., $l = 2$ or $l = 3$. The coordinates of the anchor nodes are known and fixed, which are defined as $\mathbf{X}_a = [\mathbf{x}_1, \dots, \mathbf{x}_M]_{l \times M}$, where the vector $\mathbf{x}_i = [x_{1i}, \dots, x_{li}]^T$ indicates the coordinates of the i th anchor node. A vector $\mathbf{x}(k)$ of length l denotes the unknown coordinates of the target node at time k . In an asynchronous network with clock offsets, the target node clock runs freely, and the clock skews of all the anchors are equal to 1 or treated as 1. There are only clock offsets among all the anchors. Thus, the model for the anchor clock [11] is given by $C_i(t) = t + \theta_i$, $i = 1, \dots, M$, where θ_i denotes the unknown clock offset of the i th anchor clock $C_i(t)$ relative to the absolute clock.

To make full use of the broadcast property of wireless signals, we employ the ATR protocol proposed in [5] to make all the other anchors listen to the ranging packets and record their timestamps locally, when one anchor and the target node exchange their ranging packets. This way, anchors obtain more information than for the two-way ranging (TWR) protocol proposed in the IEEE 802.15.4a standard [12] without increasing the communication load. The same packet structure as used in the standard is employed here, which is composed of a synchronization header (SHR) preamble, a physical layer header (PHR) and a data field. The first pulse of the PHR is called the ranging marker (RMARKER). The moment when the RMARKER leaves or arrives at the antenna of a node is critical to ranging. Without loss of generality, we assume that the M th anchor initiates the ATR protocol as illustrated in Fig. 1. The i th anchor records the timestamps $T_{iR}(k)$ and $T_{iS}(k)$ upon the arrival of the RMARKERS of the ranging request from the M th anchor and of the ranging response from the target node, respectively, where k is a label to indicate that

the timestamp measurements correspond to $\mathbf{x}(k)$. Note that $T_{MR}(k)$ can be interpreted as the time upon which the M th anchor receives its own ranging request without any delay, and it is recorded when the M th anchor transmits a ranging packet. Because we do not use any timestamps from the target node, the clock parameters of the target node do not have any influence on our scheme. This is an important advantage of the ATR protocol compared to the TWR protocol. For the i th anchor, the difference between $T_{iR}(k)$ and $T_{iS}(k)$ relates to the distance as

$$c(T_{iS}(k) - T_{iR}(k)) = d_i(k) + d_M(k') + \Delta(k) - d_{iM} + n_{iS}(k) - n_{iR}(k), \quad i = 1, \dots, M(1)$$

where $k' = k - \Delta(k)/c$, c is the signal propagation speed, $\Delta(k)$ is the unknown distance corresponding to the processing time of the target node, $d_i(k) = \|\mathbf{x}_i - \mathbf{x}(k)\| = \sqrt{\|\mathbf{x}_i\|^2 - 2\mathbf{x}_i^T \mathbf{x}(k) + \|\mathbf{x}(k)\|^2}$ is unknown, and $d_{ij} = \|\mathbf{x}_i - \mathbf{x}_j\|$ is known. Since the target node is moving continuously, the position where it receives the RMARKER from the M th anchor is different from the position where it sends out its RMARKER, and the time interval is the processing time $\Delta(k)/c$. Thus, the distance between the target node and the M th anchor is $d_M(k')$, when the target node receives the RMARKER from the M th anchor. As a result, there are two unknown target positions $\mathbf{x}(k)$ and $\mathbf{x}(k')$ in (1). Furthermore, $n_{iS}(k)$ and $n_{iR}(k)$ are the distance error terms translated from the measurement errors in $T_{iS}(k)$ and $T_{iR}(k)$, which can be modeled as zero mean random variables with variance $\sigma_{iS}^2(k)$ and $\sigma_{iR}^2(k)$, respectively. By making differences of the timestamps from the same anchor, the clock offsets are canceled out. Moreover, the internal delays of all the anchors except the M th anchor are also eliminated, since both $T_{iR}(k)$ and $T_{iS}(k)$ are recorded upon the arrival of the RMARKERS at the same node. The internal delay of the M th anchor can be compensated beforehand [13]. Consequently, defining $\mathbf{q} = [c(T_{1S}(k) - T_{1R}(k)), \dots, T_{MS}(k) - T_{MT}(k)]^T$, $\mathbf{d}(k) = [d_1(k), \dots, d_{M-1}(k), d_M(k)]^T$, $\mathbf{d}_a = [d_{1M}, \dots, d_{(M-1)M}, 0]^T$, $\mathbf{n}_s = [n_{1S}(k), \dots, n_{MS}(k)]^T$, and $\mathbf{n}_r = [n_{1R}(k), \dots, n_{MR}(k)]^T$, we can now write (1) in vector form as

$$\mathbf{q}(k) = \mathbf{d}(k) + (d_M(k') + \Delta(k))\mathbf{1}_M - \mathbf{d}_a + \mathbf{n}_s(k) - \mathbf{n}_r(k). \quad (2)$$

As (2) is a nonlinear model with respect to (w.r.t.) $\mathbf{x}(k)$ and $\mathbf{x}(k')$, it is impossible to derive the conventional KF for (2). Inspired by [10], we would like to linearize (2) without any approximation by projection and element-wise multiplication. We employ an orthogonal projection \mathbf{P} onto the orthogonal complement of $\mathbf{1}_M$ similarly as in [5], which is defined as $\mathbf{P} = \mathbf{I}_M - \frac{1}{M}\mathbf{1}_M\mathbf{1}_M^T$. Since $\mathbf{P}\mathbf{1}_M = \mathbf{0}_M$, \mathbf{P} can be used to eliminate the term $(d_M(k') + \Delta(k))\mathbf{1}_M$ in (2). As a result, premultiplying both sides of (2) with \mathbf{P} , we obtain $\mathbf{P}\mathbf{q}(k) = \mathbf{d}(k) - \bar{d}(k)\mathbf{1}_M + \mathbf{P}\mathbf{d}_a + \mathbf{P}\mathbf{n}_s(k) - \mathbf{P}\mathbf{n}_r(k)$, (3)

where $\mathbf{P}\mathbf{d}(k) = \mathbf{d}(k) - \bar{d}(k)\mathbf{1}_M$ with $\bar{d}(k) = \frac{1}{M}\sum_{i=1}^M d_i(k)$ being the unknown average of the distances between the target

node and the anchors. Note that (3) is now only related to $\mathbf{x}(k)$ with the penalty of losing some information due to the projection. Keeping $\mathbf{d}(k)$ on one side, moving the other terms to the other side, and making an element-wise multiplication, we can write

$$\begin{aligned} & \psi_a - 2\mathbf{X}_a^T \mathbf{x}(k) + \|\mathbf{x}(k)\|^2 \mathbf{1}_M \\ &= (\mathbf{P}(\mathbf{q}(k) + \mathbf{d}_a)) \odot (\mathbf{P}(\mathbf{q}(k) + \mathbf{d}_a)) \\ & \quad + \bar{d}^2(k) \mathbf{1}_M + 2\bar{d}(k) \mathbf{P}(\mathbf{q}(k) + \mathbf{d}_a) + \mathbf{n}(k), \end{aligned} \quad (4)$$

where $\psi_a = [\|\mathbf{x}_1\|^2, \dots, \|\mathbf{x}_M\|^2]^T$, and $\mathbf{n}(k) = -(\mathbf{P}(\mathbf{n}_s(k) - \mathbf{n}_r(k))) \odot (\mathbf{P}(\mathbf{n}_s(k) - \mathbf{n}_r(k))) - 2\bar{\mathbf{d}}(k) \odot \mathbf{P}(\mathbf{n}_s(k) - \mathbf{n}_r(k))$ with \odot denoting element-wise product. Since the unconstrained least squares (LS) estimation method is equivalent to the subspace minimization (SM) method [14], we employ the latter one in order to estimate $\mathbf{x}(k)$ alone. We first apply \mathbf{P} again to eliminate $\|\mathbf{x}(k)\|^2 \mathbf{1}_M$ and $\bar{d}^2(k) \mathbf{1}_M$, leading to

$$\begin{aligned} & \mathbf{P}\psi_a - \mathbf{P}((\mathbf{P}(\mathbf{q}(k) + \mathbf{d}_a)) \odot (\mathbf{P}(\mathbf{q}(k) + \mathbf{d}_a))) \\ &= 2\mathbf{P}\mathbf{X}_a^T \mathbf{x}(k) + 2\bar{d}(k) \mathbf{P}(\mathbf{q}(k) + \mathbf{d}_a) + \mathbf{P}\mathbf{n}(k). \end{aligned} \quad (5)$$

We then apply an orthogonal projection $\mathbf{P}_d(k)$ onto the orthogonal complement of $\mathbf{P}(\mathbf{q}(k) + \mathbf{d}_a)$ to both sides of (5), which is given by

$$\mathbf{P}_d(k) = \mathbf{I}_M - \frac{\mathbf{P}(\mathbf{q}(k) + \mathbf{d}_a)(\mathbf{q}(k) + \mathbf{d}_a)^T \mathbf{P}}{(\mathbf{q}(k) + \mathbf{d}_a)^T \mathbf{P}(\mathbf{q}(k) + \mathbf{d}_a)}. \quad (6)$$

As a result, we arrive at

$$\mathbf{b}(k) = \mathbf{F}(k)\mathbf{x}(k) + \mathbf{P}_d(k)\mathbf{P}\mathbf{n}(k), \quad (7)$$

where $\mathbf{b}(k) = \mathbf{P}_d(k)\mathbf{P}\psi_a - \mathbf{P}_d(k)\mathbf{P}((\mathbf{P}(\mathbf{q}(k) + \mathbf{d}_a)) \odot (\mathbf{P}(\mathbf{q}(k) + \mathbf{d}_a)))$ and $\mathbf{F}(k) = 2\mathbf{P}_d(k)\mathbf{P}\mathbf{X}_a^T$. Note that $\mathbf{P}_d(k)$, $\mathbf{b}(k)$ and $\mathbf{F}(k)$ all depend on time-varying measurements. We remark that in order to facilitate all the linearizations, the condition $M \geq l + 3$ has to be fulfilled, which indicates that we need at least five anchors on a plane or six anchors in space to accomplish the linearization.

Let us now explore the statistical properties of the noise. Defining $\mathbf{P}\mathbf{n}_r(k) = \mathbf{n}_r(k) - \bar{n}_r(k)\mathbf{1}_M$ and $\mathbf{P}\mathbf{n}_s(k) = \mathbf{n}_s(k) - \bar{n}_s(k)\mathbf{1}_M$, where $\bar{n}_r(k) = \frac{1}{M} \sum_{i=1}^M n_{iR}(k)$ and $\bar{n}_s(k) = \frac{1}{M} \sum_{i=1}^M n_{iS}(k)$, we can write the entries of $\mathbf{n}(k)$ as (8) on the top of the next page. Recall that $E[n_{iS}(k)] = 0$, $E[n_{iS}^2(k)] = \sigma_{iS}^2(k)$ and $E[n_{iS}(k)n_{jS}(k)] = 0, i \neq j$, which leads to $E[\bar{n}_s(k)] = 0$, $E[\bar{n}_s^2(k)] = \frac{1}{M^2} \sum_{i=1}^M \sigma_{iS}^2(k)$ and $E[\bar{n}_s(k)n_{iS}(k)] = \frac{1}{M} \sigma_{iS}^2(k)$. The statistical properties of $n_{iR}(k)$ can be obtained in a similar way. Moreover, $n_{iS}(k)$ and $n_{iR}(k), i = 1, \dots, M$ are uncorrelated. As a result, the statistical properties of $\mathbf{n}(k)$ are given by (9) and (10) on the top of the next page, where we ignore the higher order noise terms to obtain (10) and assume $E[[\mathbf{n}(k)]_i] \approx 0$ under the condition of sufficiently small measurement errors. Thus, we still treat $\mathbf{n}(k)$ as a zero mean Gaussian random vector. We remark that the noise covariance matrix depends on the unknown $\mathbf{d}(k)$. To solve this problem, we can plug in the predicted $\hat{\mathbf{d}}(k|k-1)$, which makes use of the prediction

$\hat{\mathbf{x}}(k|k-1)$ (these notations will be defined later on). Note that $\mathbf{n}(k)$ is not a stationary process but it is independent, leading to

$$\mathbf{P}_d(k)\mathbf{P}E[\mathbf{n}(k)\mathbf{n}(j)^T]\mathbf{P}\mathbf{P}_d(j) = \begin{cases} \mathbf{\Lambda}(k) & k = j \\ \mathbf{0} & k \neq j \end{cases}, \quad (11)$$

where $\mathbf{\Lambda}(k)$ is rank-deficient due to the projections.

3. DYNAMIC STATE MODEL AND KALMAN FILTER

Let us define the state at time k as $\mathbf{s}(k) = [\mathbf{x}(k)^T, \dot{\mathbf{x}}(k)^T, \ddot{\mathbf{x}}(k)^T]^T$, where $\mathbf{x}(k)$, $\dot{\mathbf{x}}(k)$ and $\ddot{\mathbf{x}}(k)$ are the coordinate, the velocity and the acceleration vectors of the target node at time k , respectively. We assume a general linear state model, which is given by (see also [6])

$$\mathbf{s}(k+1) = \mathbf{A}(k)\mathbf{s}(k) + \mathbf{B}(k)\mathbf{u}(k) + \mathbf{w}(k), \quad (12)$$

where $\mathbf{A}(k)$ is a $3l \times 3l$ state transition matrix, $\mathbf{B}(k)$ is a $3l \times l$ input matrix, $\mathbf{u}(k)$ is an acceleration input vector of length l , and $\mathbf{w}(k)$ is a driving noise vector of length l with zero mean and a covariance matrix $\mathbf{R}(k)$, which is given by

$$E[\mathbf{w}(k)\mathbf{w}(j)^T] = \begin{cases} \mathbf{R}(k) & k = j \\ \mathbf{0} & k \neq j \end{cases}. \quad (13)$$

We assume that $\mathbf{A}(k)$, $\mathbf{B}(k)$ and $\mathbf{u}(k)$ are all known exactly. Moreover, the driving noise and the measurement noise are assumed independent. In practice, $\mathbf{u}(k)$ has to be estimated first. In [15] for instance, $\mathbf{u}(k)$ is modeled as a semi-Markov process with a finite number of possible acceleration inputs, which are selected based on the transition probabilities of a Markov process. As a result, $\mathbf{u}(k)$ can be estimated by a minimum mean square error (MMSE) estimator. On the other hand, [16] does not require a statistical model for $\mathbf{u}(k)$, and derives a LS estimator of $\mathbf{u}(k)$.

Let us now rewrite the measurement model (7) using $\mathbf{s}(k)$ as

$$\mathbf{b}(k) = \mathbf{C}(k)\mathbf{s}(k) + \mathbf{P}_d(k)\mathbf{P}\mathbf{n}(k), \quad (14)$$

where $\mathbf{C}(k) = [\mathbf{F}(k), \mathbf{0}_{M \times 2l}]$. Based on (12) and (14), we can easily develop the corresponding KF tracker. The prediction equations are given by

$$\begin{aligned} \hat{\mathbf{s}}(k|k-1) &= \mathbf{A}(k-1)\hat{\mathbf{s}}(k-1|k-1) + \mathbf{B}(k-1)\mathbf{u}(k-1), \\ \mathbf{P}_s(k|k-1) &= \mathbf{A}(k-1)\mathbf{P}_s(k-1|k-1)\mathbf{A}(k-1)^T + \mathbf{R}(k-1). \end{aligned} \quad (15)$$

The update equations are given by

$$\mathbf{K}(k) = \mathbf{P}_s(k|k-1)\mathbf{C}(k)^T (\mathbf{C}(k)\mathbf{P}_s(k|k-1)\mathbf{C}(k)^T + \mathbf{\Lambda}(k))^\dagger, \quad (17)$$

$$\hat{\mathbf{s}}(k|k) = \hat{\mathbf{s}}(k|k-1) + \mathbf{K}(k)(\mathbf{b}(k) - \mathbf{C}(k)\hat{\mathbf{s}}(k|k-1)), \quad (18)$$

$$\mathbf{P}_s(k|k) = (\mathbf{I}_M - \mathbf{K}(k)\mathbf{C}(k))\mathbf{P}_s(k|k-1). \quad (19)$$

Note that since $\mathbf{C}(k)\mathbf{P}_s(k|k-1)\mathbf{C}(k)^T + \mathbf{\Lambda}(k)$ may be rank-deficient, we use the pseudo-inverse instead of the inverse, which is denoted here by $(\cdot)^\dagger$.

$$[\mathbf{n}(k)]_i = 2d_i(n_{iR}(k) - \bar{n}_r(k) - n_{iS}(k) + \bar{n}_s(k)) - (n_{iR}(k) - \bar{n}_r(k) - n_{iS}(k) + \bar{n}_s(k))^2, i=1, 2, \dots, M. \quad (8)$$

$$E[[\mathbf{n}(k)]_i] = \frac{2-M}{M}(\sigma_{iR}^2(k) + \sigma_{iS}^2(k)) - \frac{1}{M^2} \sum_{p=1}^M (\sigma_{pR}^2(k) + \sigma_{pS}^2(k)) \approx 0, \quad (9)$$

$$E[[\mathbf{n}(k)]_i[\mathbf{n}(k)]_j] \approx \begin{cases} 4d_i(k)^2 \left(\frac{M-2}{M}(\sigma_{iR}^2(k) + \sigma_{iS}^2(k)) + \frac{1}{M^2} \sum_{p=1}^M (\sigma_{pR}^2(k) + \sigma_{pS}^2(k)) \right), & i=j \\ 4d_i(k)d_j(k) \left(\frac{1}{M^2} \sum_{p=1}^M (\sigma_{pS}^2(k) + \sigma_{pR}^2(k)) - \frac{1}{M}(\sigma_{iS}^2(k) + \sigma_{jS}^2(k) + \sigma_{iR}^2(k) + \sigma_{jR}^2(k)) \right), & i \neq j \end{cases} \quad (10)$$

4. EXTENDED KALMAN FILTER

In this section, we derive the EKF as a benchmark for our KF tracker. In order to apply the EKF, we first have to use a Taylor expansion to linearize the nonlinear measurement model. Recall the data model (3) here, which is the result of applying the projection \mathbf{P} to (2) in order to get rid of the dominant term $(d_M(k') + \Delta(k))\mathbf{1}_M$, where $\Delta(k)$ is the unknown distance corresponding to the processing time, and $d_M(k')$ is the distance between $\mathbf{x}(k')$ and the M th anchor. As a result of the projection, (3) is only related to $\mathbf{x}(k)$:

$$\mathbf{P}\mathbf{q}(k) = \mathbf{d}(k) - \bar{d}(k)\mathbf{1}_M - \mathbf{P}\mathbf{d}_a + \mathbf{P}(\mathbf{n}_s(k) - \mathbf{n}_r(k)), \quad (20)$$

where we recall that $\bar{d}(k) = \frac{1}{M} \sum_{i=1}^M d_i(k)$. Let us define the function $f(\mathbf{x}(k))$ as $f(\mathbf{x}(k)) = \mathbf{d}(k) - \bar{d}(k)\mathbf{1}_M - \mathbf{P}\mathbf{d}_a(k)$, where we recall that $d_i(k) = \|\mathbf{x}(k) - \mathbf{x}_i(k)\|$. The Jacobian $\mathbf{H}(k)$ of $f(\mathbf{x}(k))$ w.r.t. $\mathbf{s}(k)$ can be expressed as

$$\begin{aligned} [\mathbf{H}(k)]_{i,j} &= \left. \frac{\partial [f(\mathbf{x}(k))]_i}{\partial [\mathbf{s}(k)]_j} \right|_{\mathbf{s}(k)=\hat{\mathbf{s}}(k|k-1)}, \quad \text{with} \\ \frac{\partial [f(\mathbf{x}(k))]_i}{\partial \mathbf{x}(k)} \bigg|_{\mathbf{x}(k)=\hat{\mathbf{x}}(k|k-1)} &= \left(\frac{(\mathbf{x}(k) - \mathbf{x}_i(k))^T}{\|\mathbf{x}(k) - \mathbf{x}_i(k)\|} \right. \\ &\quad \left. - \frac{1}{M} \sum_{j=1}^M \frac{(\mathbf{x}(k) - \mathbf{x}_j(k))^T}{\|\mathbf{x}(k) - \mathbf{x}_j(k)\|} \right) \bigg|_{\mathbf{x}(k)=\hat{\mathbf{x}}(k|k-1)}, \quad (21) \end{aligned}$$

$$\begin{aligned} \frac{\partial [f(\mathbf{x}(k))]_i}{\partial \hat{\mathbf{x}}(k)} \bigg|_{\hat{\mathbf{x}}(k)=\hat{\mathbf{x}}(k|k-1)} &= \frac{\partial [f(\mathbf{x}(k))]_i}{\partial \mathbf{x}(k)} \bigg|_{\mathbf{x}(k)=\hat{\mathbf{x}}(k|k-1)} \\ &= \mathbf{0}_l^T. \quad (22) \end{aligned}$$

Recall that $\mathbf{n}_s(k)$ and $\mathbf{n}_r(k)$ are zero mean independent Gaussian random variables with variance $\sigma_{iS}^2(k)$ and $\sigma_{iR}^2(k)$, respectively. Defining $\tilde{\mathbf{\Lambda}}(k)$ as the noise covariance matrix of the noise term $\mathbf{P}(\mathbf{n}_s(k) - \mathbf{n}_r(k))$, which is a zero mean Gaussian random vector, we can write $\tilde{\mathbf{\Lambda}}(k) = \mathbf{P}\text{diag}([\sigma_{1S}^2(k) + \sigma_{1R}^2(k), \dots, \sigma_{MS}^2(k) + \sigma_{MR}^2(k)])\mathbf{P}$.

Consequently, the EKF is developed as follows. The prediction equations are the same as (15) and (16). The update equations are

$$\tilde{\mathbf{K}}(k) = \tilde{\mathbf{P}}_s(k|k-1)\mathbf{H}(k)^T(\mathbf{H}(k)\tilde{\mathbf{P}}_s(k|k-1)\mathbf{H}(k)^T + \tilde{\mathbf{\Lambda}}(k))^{-1},$$

$$\begin{aligned} \hat{\mathbf{s}}(k|k) &= \hat{\mathbf{s}}(k|k-1) + \tilde{\mathbf{K}}(k)(\mathbf{P}\mathbf{q}(k) - f(\hat{\mathbf{x}}(k|k-1))), \\ \tilde{\mathbf{P}}_s(k|k) &= (\mathbf{I}_M - \tilde{\mathbf{K}}(k)\mathbf{H}(k))\tilde{\mathbf{P}}_s(k|k-1). \end{aligned}$$

5. SIMULATION RESULTS

Let us now evaluate the performance of the proposed KF tracker by Monte Carlo simulations, and compare it with the EKF. We consider a simulation setup, where the first anchor is located at the origin, and the other four anchors are located at the corners of a $100 \text{ m} \times 100 \text{ m}$ rectangular centered around the origin. Due to the broadcast nature of the ATR protocol, we assume that $\sigma_{iS}^2(k)$ and $\sigma_{iR}^2(k)$ are related to the distances according to the path loss law. Thus we define the average noise power as $\bar{\sigma}^2 = 1/M \sum_{i=1}^M \sigma_{iS}^2(k)$, where $\sigma_{iR}^2(k)$ and $\sigma_{iS}^2(k)$ are chosen to fulfill the condition that all $\sigma_{iR}^2(k)/d_{iM}^2$ and $\sigma_{iS}^2(k)/d_i^2(k)$ are equal. Note that since $d_{MM} = 0$, we simply assume $\sigma_{MR}^2(k) = 0$ and $n_{MR} = 0$. The processing time of the target node is 5 ms, and the signal propagation speed c is the speed of the light. As a result the corresponding distance $\Delta(k)$ is $3 \times 10^8 \times 5 \times 10^{-3} = 1.5 \times 10^6 \text{ m}$, which is much larger than the scale of the considered set-up. We employ a random walk state model as in [17], where (12) is reduced to

$$\mathbf{s}(k+1) = \begin{bmatrix} \mathbf{I}_l & T_s \mathbf{I}_l & \mathbf{0}_{l \times l} \\ \mathbf{0}_{l \times l} & \mathbf{I}_l & \mathbf{0}_{l \times l} \\ \mathbf{0}_{l \times l} & \mathbf{0}_{l \times l} & \mathbf{0}_{l \times l} \end{bmatrix} \mathbf{s}(k) + \begin{bmatrix} \mathbf{0}_l \\ \mathbf{w}_{\hat{\mathbf{x}}}(k) \\ \mathbf{0}_l \end{bmatrix}, \quad (26)$$

where $\mathbf{w}_{\hat{\mathbf{x}}}(k)$ is a zero mean white random process with covariance matrix $\sigma_w^2 \mathbf{I}_l$, and T_s is the sampling interval. For a true initial state $\mathbf{s}(-1) = [\mathbf{x}(-1)^T, \mathbf{v}(-1)^T, \mathbf{0}_l^T]^T$, the initial state estimate $\hat{\mathbf{s}}(-1|-1)$ is randomly generated in each Monte Carlo run according to $\mathcal{N}(\mathbf{s}(-1), \mathbf{P}_s(-1|-1))$, with $\mathbf{P}_s(-1|-1) = 100\text{diag}([\mathbf{1}_l^T, \mathbf{1}_l^T, \mathbf{0}_l^T]^T)$. The same initial state estimate is also used for the EKF. In each run, we generate a trajectory of 100 points based on the state model. The performance criterion is the root mean square error (RMSE) of $\hat{\mathbf{x}}$ (or $\hat{\mathbf{x}}$) vs. the time index k , which can be expressed as $\sqrt{1/N_{exp} \sum_{j=1}^{N_{exp}} \|\hat{\mathbf{x}}(j) - \mathbf{x}\|^2}$, where $\hat{\mathbf{x}}(j)$ is the estimate obtained in the j th trial. Each simulation result is averaged over $N_{exp} = 500$ Monte Carlo trials. The rest of the parameters are given by $\mathbf{x}(-1) = [13 \text{ m}, 4 \text{ m}]^T, \mathbf{v}(-1) = [0.05 \text{ m/s}, -0.05 \text{ m/s}]^T, T_s = 1 \text{ s}, \sigma_{\hat{\mathbf{x}}}^2 = \sigma_{\mathbf{x}}^2 = \sigma_w^2 = 0.01, 1/\bar{\sigma}^2 = 20 \text{ dBm}$.

Fig. 2 shows an example of the trajectories estimated (23) by the proposed KF (the line with “+” markers) and the (24) EKF (the line with “x” markers), respectively. The true trajectory is the line with “o” markers. Fig. 3(a) illus-

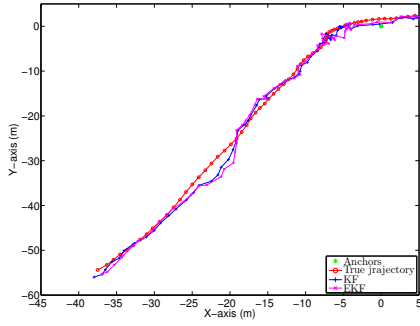
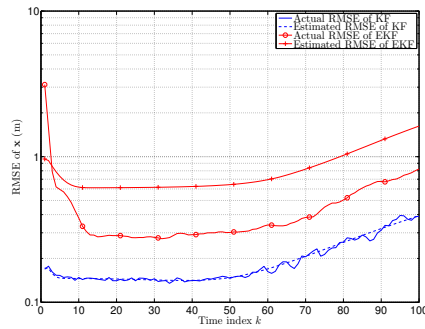
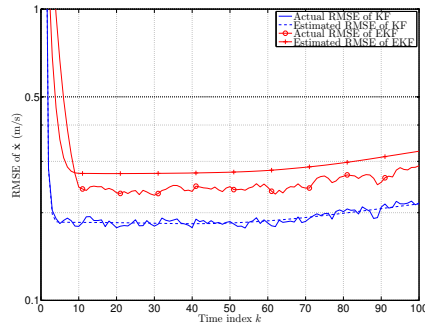


Fig. 2. An example of the trajectories estimated by the proposed KF and the EKF



(a) RMSE of the target node location \mathbf{x} vs. time index k



(b) RMSE of the target node velocity $\dot{\mathbf{x}}$ vs. time index k

Fig. 3. RMSE of the proposed KF and the EKF

trates the performance of the position estimate $\hat{\mathbf{x}}$ by the proposed KF and the EKF, respectively. The proposed KF achieves better accuracy than the EKF. Both RMSEs increase with time, since the covariance matrix of the state also increases with time. Furthermore, the true RMSE (the solid line) of the proposed KF closely follows its estimated RMSE (the dashed line), which is calculated by $\sqrt{1/N_{exp} \sum_{j=1}^{N_{exp}} ([\mathbf{P}^{(j)}(k|k)]_{1,1} + [\mathbf{P}^{(j)}(k|k)]_{2,2})}$ with $\mathbf{P}^{(j)}(k|k)$ the covariance estimate obtained in the j th trial. On the other hand, the true RMSE (the solid line with “o” markers) of the EKF is below its estimated RMSE (the solid line with “+” markers), which shows that the estimated RMSE of the EKF

is pessimistic. We observe the same tendency in Fig. 3(b), which illustrates the performance of the velocity estimate $\hat{\dot{\mathbf{x}}}$ by the proposed KF and the EKF, respectively.

6. REFERENCES

- [1] K. Yu, J. philippe Montillet, A. Rabbachin, P. Cheong, and I. Oppermann, “UWB location and tracking for wireless embedded networks,” *Signal Processing*, vol. 86, no. 9, pp. 2153–2171, 2006.
- [2] T. Li, A. Ekpenyong, and Y.-F. Huang, “Source localization and tracking using distributed asynchronous sensors,” *IEEE Trans. Signal Process.*, vol. 54, no. 10, pp. 3991–4003, 2006.
- [3] M. Vemula, J. Miguez, and A. Artes-Rodriguez, “A sequential monte carlo method for target tracking in an asynchronous wireless sensor network,” in *Proc. WPNC*, Mar. 2007, pp. 49–54.
- [4] S. Gezici, Z. Tian, G. Giannakis, H. Kobayashi, A. Molisch, H. Poor, and Z. Sahinoglu, “Localization via ultra-wideband radios: a look at positioning aspects for future sensor networks,” *IEEE Signal Process. Mag.*, vol. 22, pp. 70–84, July 2005.
- [5] Y. Wang, G. Leus, and X. Ma, “Time-based localization for asynchronous wireless sensor networks,” in *Proc. IEEE ICASSP*, Prague, Czech Republic, May 2011, accepted.
- [6] Y. Shalom, X. Li, and K. T., *Estimation with applications to tracking and navigation*. New York: Wiley, 2001.
- [7] S. Julier and J. Uhlmann, “Unscented filtering and nonlinear estimation,” *Proceedings of the IEEE*, vol. 92, no. 3, pp. 401–422, Mar. 2004.
- [8] F. Gustafsson, F. Gunnarsson, N. Bergman, U. Forssell, J. Jansson, R. Karlsson, and P.-J. Nordlund, “Particle filters for positioning, navigation, and tracking,” *IEEE Trans. Signal Process.*, vol. 50, no. 2, pp. 425–437, Feb. 2002.
- [9] B. R. Hamilton, X. Ma, Q. Zhao, and J. Xu, “ACES: adaptive clock estimation and synchronization using Kalman filtering,” in *MobiCom ’08*. New York, NY, USA: ACM, 2008, pp. 152–162.
- [10] R. Doraiswami, “A novel Kalman filter-based navigation using beacons,” *IEEE Trans. Aerosp. Electron. Syst.*, vol. 32, no. 2, pp. 830–840, 1996.
- [11] B. Sundararaman, U. Buy, and A. Kshemkalyani, “Clock synchronization for wireless sensor networks: a survey,” *Ad Hoc Networks*, vol. 3, no. 3, pp. 281–323, Jan. 2005.
- [12] IEEE Working Group 802.15.4, “Part 15.4: Wireless medium access control (MAC) and physical layer (PHY) specifications for low-rate wireless personal area networks (WPANs),” Tech. Rep., 2007.
- [13] K. Yu, Y. Guo, and M. Hedley, “TOA-based distributed localisation with unknown internal delays and clock frequency offsets in wireless sensor networks,” *IET Signal Processing*, vol. 3, no. 2, pp. 106–118, 2009.
- [14] P. Stoica and J. Li, “Lecture notes - source localization from range-difference measurements,” *IEEE Signal Process. Mag.*, vol. 23, no. 6, pp. 63–66, Nov. 2006.
- [15] R. Moose, H. Vanlandingham, and D. McCabe, “Modeling and estimation for tracking maneuvering targets,” *IEEE Trans. Aerosp. Electron. Syst.*, vol. 15, no. 3, pp. 448–456, May 1979.
- [16] Y. Chan, A. Hu, and J. Plant, “A Kalman filter based tracking scheme with input estimation,” *IEEE Trans. Aerosp. Electron. Syst.*, vol. 15, no. 2, pp. 237–244, Mar. 1979.
- [17] S. Kay, *Fundamentals of Statistical Singal Processing – Estimation Theory*. Englewood Cliffs, NJ: Prentice-Hall, 1993.